New insights into cryogenic and TESPEL pellet physics in TJ-II

D. Medina-Roque[1*], I. García-Cortés[1], K. J. McCarthy[1], N. Tamura[2], N. Panadero[1], E. Ascasíbar[1], T. Estrada[1], J. Hernández-Sánchez[1], A. S. Kozachek[3], M. Liniers[1], P. Medina[1], M. A. Ochando[1], J. L. de Pablos[1], I. Pastor[1], C. Toledo[4], B. van Milligen[1] & TJ-II team[1]

[1]*Laboratorio Nacional de Fusión, CIEMAT, Madrid, Spain*
[2]*National Institute for Fusion Science, Toki, Japan*
[3]*Institute of Plasma Physics, NSC KIPT Kharkov, Ukraine*
[4]*Facultad de Ciencias Físicas, Universidad Complutense de Madrid, Madrid, Spain*

Introduction

Cryogenic and tracer pellet injectors are operated on many magnetic confinement devices to identify and study scenarios to achieve efficient core fueling and avoid impurity accumulation. Both system types are available in the stellarator TJ-II alongside a wide variety of diagnostics to study pellet physical processes and post-injection plasma response, e.g., a dual HIBP system, magnetic-coil arrays, a 2-channel Doppler reflectometer and a high-resolution Thomson scattering system [1]. Here, details of the injections experiments and findings, plus their implications for pellet injection physics, are presented and discussed.

Experimental set-up

TJ-II is a 4-period medium-size heliac-type stellarator with major radius of 1.5 m, averaged minor radius a ≤0.2 m and magnetic field B_0 ≤1.1 T. Hydrogen plasmas are heated using 2 gyrotrons operated at 53.2 GHz (P_{ECRH} ≤500 kW, t_{ECRH} ≤300 ms) allowing central electron densities, n_{e0}, and electron and ion temperatures, T_{e0} and T_{i0}, up to 1.7×10^{19} m^{-3} and 1 keV and 90 eV, respectively [2]. Additional heating is supplied by 2 tangential NBI systems (P_{NBI} ≤1 MW, t_{NBI} ≤120 ms), which inject anti-parallel and parallel to the toroidal magnetic field direction, allowing n_{e0}, T_{e0} and T_{i0} up to ~8×10^{19} m^{-3}, 400 and 130 eV, respectively, to be achieved. A pipe-gun type cryogenic PI, fitted with fast-valve gas propellant systems, allows in-situ fabrication of up to 4 hydrogen pellets (0.4 to 3×10^{19} H per pellet). Thus, pellets are injected from the outer plasma edge at velocities from 800 to 1200 m/s and with separation times between pellets of ≥1 ms into both ECRH and NBI heated phases of the plasmas. A TESPEL system is attached to upstream end of one of the pellet tubes [3]. This means that TESPELs, with 300 μm diameter and containing a selected tracer, can be injected in to the same TJ-II sector at velocities between 200 and 400 m/s. Finally, TJ-II is also equipped with a wide set of diagnostics of interest for this study [1].

Results

Pellet injections into TJ-II are characterized by abrupt drops in core T_e and Hα light emission. In addition, a transitory reduction of broadband magnetic fluctuations, as measured by

Mirnov coils, is seen. This is attributed to plasma cooling. Looking more closely at magnetic signals during cryogenic pellet injections, magnetic instabilities occur near the end of the pellet ablation phase for both ECRH and NBI heated plasmas [4]. This is attributed to the outward drifting of plasmoids, that detach from the ablating pellet when it is in the plasma core region, interacting with an 8/5 rational surface located at r/a = 0.75. Abrupt plasmoid deceleration can occur as external electric potential reconnection lengths of plasmoids are significantly reduced in the vicinity of such a flux surface. Next, the deposition of the cold high-density plasmoid leads to an abrupt steepening of the local radial pressure gradient. This in turn gives rise to a magnetic instability that leads to a local magnetic field variation. Such instabilities are short lived and magnetic reconstruction occurs once homogenization is completed. In the case of TESPELS (-C_8H_8-), reduced outward drifting due to the higher ion mass means that the plasmoids are deposited in the plasma before reaching the same rational surface [5]. These experimental observations agree with predictions from the HPI2 code [6].

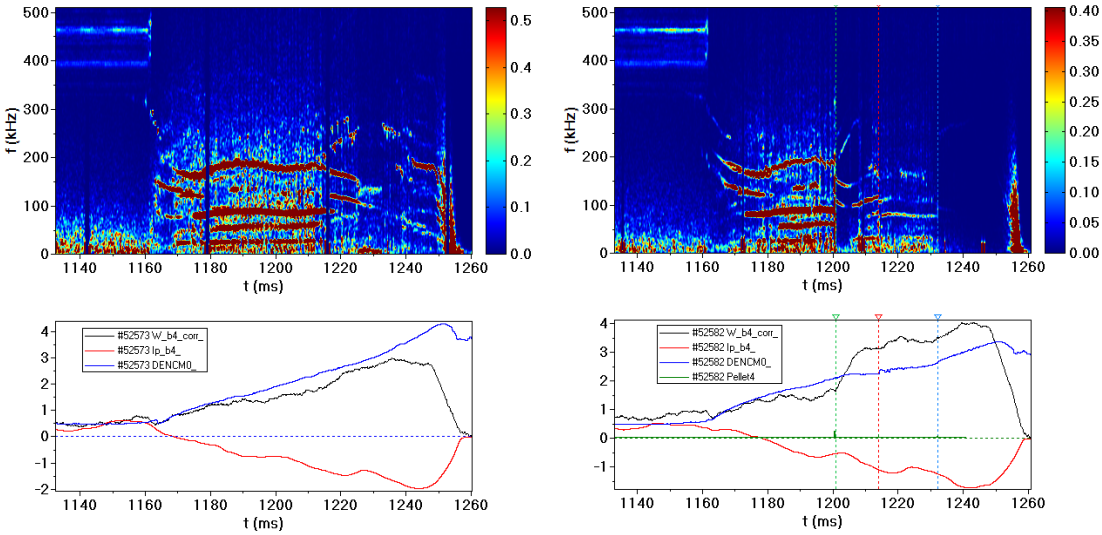

Figure 1. Top: Spectrographs of density turbulence along two TJ-II discharges as measured by the HIBP beam current signal when this is set at r/a = 0.5. The colour bar represents signal intensity. Bottom: Diamagnetic plasma energy (black), plasma line-averaged density (blue) and plasma current (red) for reference discharge #52573 (Left) and discharge #52582 with 3 pellets injected (Right), at ~1200 ms, ~1214 ms and ~1232 ms.

In experiments performed with multiple cryogenic pellets into NBI heated discharges, density turbulence, as measured with a HIBP beam set at r/a = 0.5, is suppressed after a first large pellet is injected. The turbulence has recovered partially when a smaller pellet is injected. It is then totally reduced when a second small pellet is injected, see Fig. 1. These pellet injections result in a Pellet-induced Enhanced Confinement (PiEC) phase. It is considered that turbulence suppression at this radius can be correlated with the observed increase in plasma diamagnetic energy.

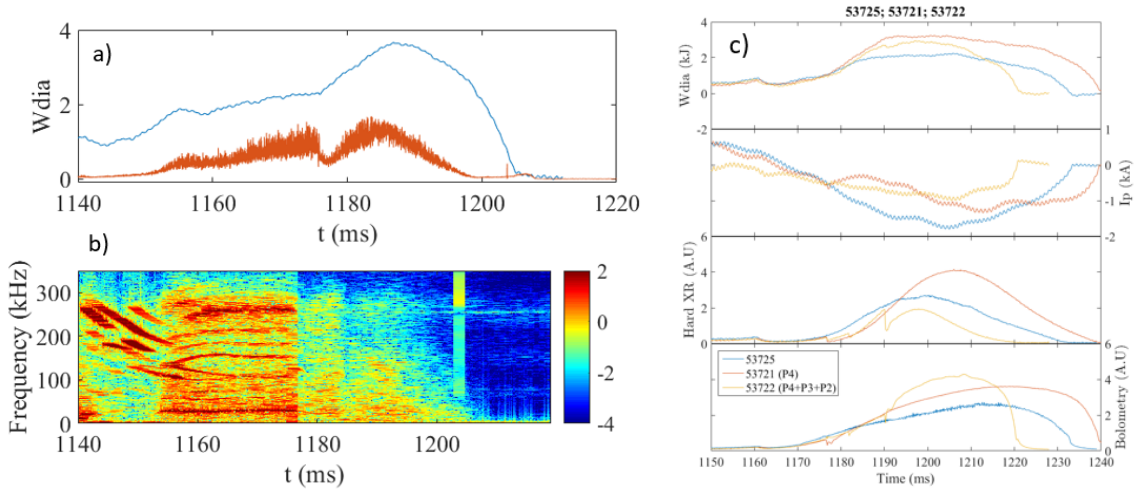

Figure 2. a) Plasma diamagnetic energy (blue) and fast-ion loss flux (brown) as measured by a Fast-Ion Loss Probe along discharge #53891. b) Spectrograph of magnetic fluctuations measured by a Mirnov Coil for the same discharge. The colour bar represents the log10 of signal intensity. c) Diamagnetic energy (kJ), Plasma current (kA), soft X-ray emission and bolometer radiation measurements for discharge #53725 (blue without PI), #53721 with 1 pellet (red) and #53722 with 3 pellets (yellow).

An additional effect observed after cryogenic PI into NBI heated plasma is a reduction of the fast-ion flux escaping the plasma. See Fig 2. This may be related to the suppression and frequency shift of the Alvén eigenmode activity observed by the Mirnov coils. Moreover, PIs can also have a significant effect on the evolution of plasma current (see Fig 3c) thus, they can have an impact on the central plasma iota. However, a full understanding of the post-injection reduction of the fast-ion flux reduction and post-injection evolution of plasma current remains outstanding at present.

Next, cryogenic pellets injection into TJ-II plasmas has also allowed the radial localization of magnetic islands to be determined. See Figure 3. In the examples, a pellet is injected along a flight path (P3) that intersects the 8/5 rational surface at r/a = ~0.4. A significant reduction is seen in the Hα emission light signal of the ablation profile as a pellet crosses this surface (see Fig. 3). This is believed to be caused by a local reduction in electron temperature and density within this island as these parameters are the main contributors to the pellet ablation process. Note: when a pellet is injected along the P2 path, no reduction is seen in Hα light. In this case, the pellet passes close to, but not through the 8/5 surface. In contrast, the ablation process is much weaker at r/a = 0.9, where a 3/2 rational surface is located, to be able to detect any changes in light emission as a pellet intersects it.

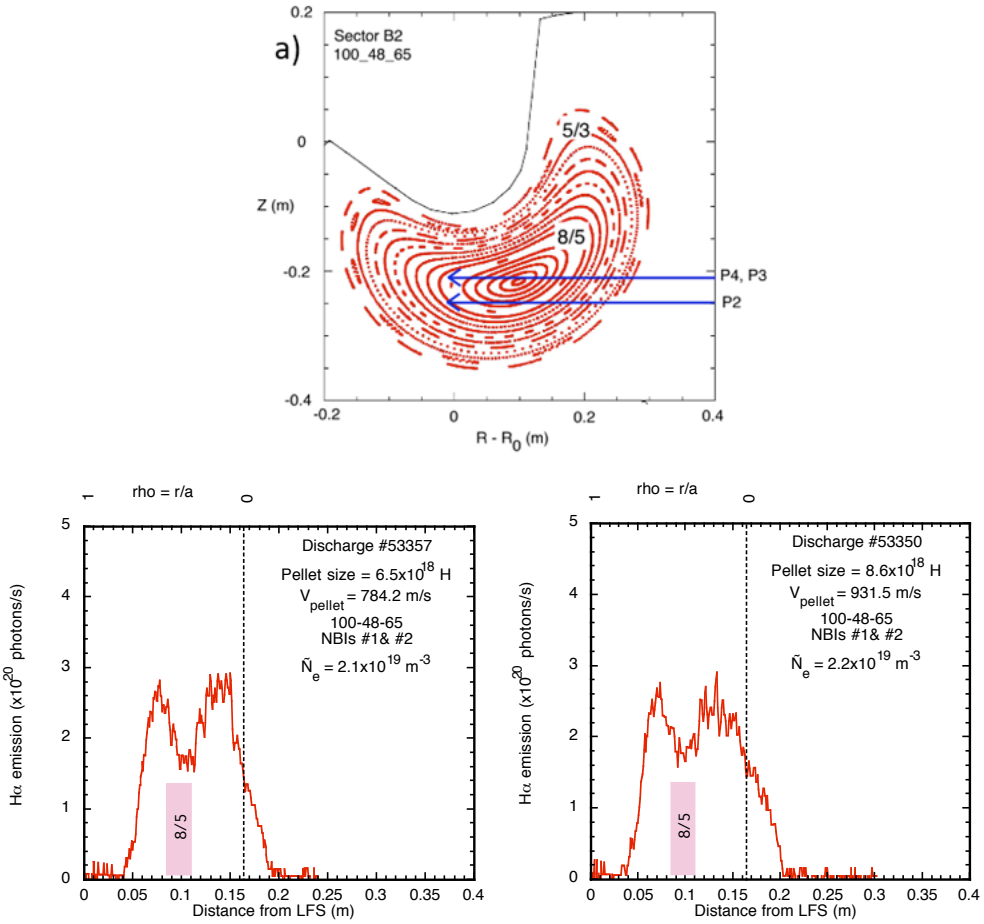

Figure 3. Top) Cross-sectional cut, in the PI sector of TJ-II, showing a Poincaré plot of closed magnetic flux surfaces for configuration 100_48_65. This configuration has rational surfaces, $\iota/2\pi$ = 8/5 and 3/2, located at r/a = 0.4 and 0.9, respectively. Flight paths (blue) are shown for pellets that pass through the magnetic axis (P4, P3) and that have nearest approach to the magnetic axis at r/a=0.3 (P2). Bottom) Hα ablation light signals for a pellet injected along flight path P3 into discharges #53350 and #53357, respectively. The location of the 8/5 rational surface along the flight path is indicated. These discharges were heated using both NBI systems.

This work has been carried out within the framework of the EUROfusion Consortium, funded by the European Union via the Euratom Research and Training Programme (Grant Agreement No 101052200 - EUROfusion). Views and opinions expressed are however those of the author(s) only and do not necessarily reflect those of the European Union or the European Commission. Neither the European Union nor the European Commission can be held responsible for them. In addition, it is partially financed by grants from the Spanish Ministerio de Ciencia e Innovación (PID2020-116599RB-I00). The authors acknowledge the contributions to data collection, analysis and interpretation made by A. Melnikov, M. Drabinskiy, L. G. Eliseev, and P. Khabanov.

[1] K. J. McCarthy, J. Instrum. 16 (2021) C12026.
[2] C. Hidalgo et al., Nucl. Fusion 62 (2022) 042025.
[3] K. J. McCarthy et al., Europhys. Lett. 120 (2017) 25001.
[4] K. J. McCarthy et al., Nucl. Fusion 61 (2021) 076014.
[5] A. Matsuyama et al., Plasma Fusion Res. Lett. 7 (2012) 1303006.
[6] N. Panadero et al., Nucl. Fusion 58 (2018) 026025.